XL CILAMCE
IBERO-LATIN AMERICAN CONGRESS ON COMPUTATIONAL METHODS IN ENGINEERING
NOVEMBER 11-14, 2019
Praiamar Natal Hotel & Convention Natal, RN-BRAZIL

MICROMECHANICS-BASED CRITERION FOR MICRO-FRACTURE PROPAGATION IN VISCOELASTIC MATERIALS

Cássio B. Aguiar
Samir Maghous
cassio.barros.aguiar@gmail.com
samir.maghous@ufrgs.br
Department of Civil Engineering, Federal University of Rio Grande do Sul
Av. Osvaldo Aranha, 99, 90035-190 Porto Alegre-RS, Brazil

Abstract. Most of engineering materials exhibit natural or load-induced fractures, which strongly affect both the instantaneous and delayed mechanical behaviors at macroscopic level. Unlike cracks, fractures are mechanically regarded as interfaces able to transfer normal and tangential efforts. The aim of this paper is to formulate the conditions for fracture propagation in randomly-micro-fractured viscoelastic materials. The homogenized viscoelastic relaxation tensor was formulated by applying the correspondence principle upon the already-known homogenized elastic stiffness tensor. Extending the Griffith-like thermodynamic framework to the macroscopic viscoelastic context, the propagation criterion is first formulated, once again comparing the energy release rate to the critical energy. Mathematical evidences shows the energy release rate is written as the derivative of the macroscopic elastic energy, written to the viscoelasticity, with respect to the parameter which represents the damage in the macroscopic scale. Under certain conditions, the elastic energy derivative can be simplified, being reduced only to an instantaneous term, leading to a simplified propagation criterion. It was notably found that for constant strain loadings, the fracture propagation is exactly driven by elastic components. Analyses performed for constant strain rates on specimen made of Burger solid matrix show that the energy release rate increases from zero to a constant asymptotic value. This asymptotic energy release rate is used in a time-independent propagation criterion, evidencing an interval to initial damage parameter where the propagation is possible. The main contribution of asymptotic energy release rate, however, refers to the estimative of final damage parameter after the end of propagation.

Keywords: Propagation Criterion, Viscoelasticity, Micromechanics, Homogenization, Fractures

1 Introduction

As far as the engineers have been refining their projects, introducing news analysis models, some material characteristics, previously neglected, become indispensable. When damaged materials are loaded, existing discontinuities are expected to grow and propagate, increasing their size and number. From the physical viewpoint, two classes of discontinuities are distinguished: cracks and fractures. Although both are generally modeled through interfaces, the intrinsic capacity associated with fractures, referring to the transmission of normal and tangential stresses along their length, makes their modeling much more similar to reality. Referring to propagation studies, linear or non-linear mechanisms have been applied since the pioneering work of Griffith, giving less attention, however, to the evaluation of propagation of discontinuities able of transferring efforts.

In this respect, most of the theoretical or computational analysis has focused on the instantaneous (elastic and plastic) material response. However, in many situations, the deferred behavior proves to be a fundamental component of the material deformation, making it indispensable for the analysis of propagation. Unlike elastic or plastic structures, it is expected that the propagation criterion depends directly on the time. Criteria for propagation of cracks have been addressed in the viscoelasticity referring to single discontinuity [7-14]. However, these approaches are difficult to implement in engineering applications involving a large number of micro-fractures.

More recent approaches [15,16] based on micromechanics theory have extended Griffith's elastic thermodynamic reasoning to the viscoelastic context, allowing the formulation of a propagation criterion for micro-cracked materials associated with a variable which represents the damage on a macroscopic scale. The objective of this work is to extend the existing reasoning to discontinuities able of transferring stresses (i.e. fractures), formulating a fracture propagation condition for viscoelastic materials.

This work is divided into three parts. The first one dealing with the homogenization of the fractured viscoelastic material properties, the second one referring to the propagation criterion, developed by mean of thermodynamic laws in a similar way than Griffith's woks. In the third part, numerical applications are performed, allowing the reasoning for propagation start time. Analysis to constant strain rate loadings lead the energy release rate to an asymptotic-in-time value, which is used to determine the interval for initial damage parameter where the damage propagate. The main contribution of the asymptotic value refers to the energy release rate/critical energy balance that, supposing mechanical equilibrium during the fracture evolution, leads to a minimum estimative for the final damage parameter after the fracture propagation is finished. In addition, alternative propagation conditions focused on strains and stresses are presented, allowing the development of propagation analysis based on loadings or requesting efforts.

2 Homogenized viscoelastic mechanical behavior

The viscoelastic damage propagation analysis, formulated in the context of micromechanics theory, requests the viscoelastic fractured effective behavior. The effective behavior, also referred as homogenized behavior, can be accessed through elastic homogenization schemes combined to the Laplace-Carson correspondence principle. Using Eshelby-based schemes, Aguiar and Maghous [1] determined the homogenized behavior considering both viscoelastic matrix and fractures. The following reasoning explain the context where the effective behavior was formulated as well as present the equations that describes the isotropic resultant relaxation tensor.

Considering that natural fractures are randomly distributed on the medium, the micromechanics theory determine the material can be statistically represented by means of a representative elementary volume (REV) whenever specific scale separations conditions are satisfied. That conditions can be summarized as $d \ll l \ll L$, where d stands for the average heterogeneities length, l is the REV length and L represents the structure characteristic length. In the subsequent analysis Ω denotes the

REV composed by the solid matrix and fractures, ω is the volume occupied by all fractures and $\Omega \setminus \omega$ stands for the solid matrix phase, corresponding to the REV without the fractures.

Each fracture is modeled as an interface geometrically described by a surface ω_i, related to its normal orientation vector $\underline{n}_i$. At a smaller scale however, the fracture would be represented by a finite-thickness volume delimited by distinct upper ω_i^+ and lower ω_i^- boundaries (see Figure 1). The main difference between cracks and fractures refers to the fracture's stress transfer ability, correlating stress forces $\underline{T} = \underline{\underline{\sigma}} \cdot \underline{n}$ (acting in the discontinuity interface) and displacements jumps $\left[\!\left[\underline{\xi} \right]\!\right] = \underline{\xi}^+ - \underline{\xi}^-$ (along the discontinuity length) over the fracture stiffness $\underline{\underline{k}}$ (for more details see Goodman [2] or Bandis et al. [3]). On the elastic scope that relationship is given by:

$$\underline{T} = \underline{\underline{k}} : \left[\!\left[\underline{\xi} \right]\!\right] \tag{1}$$

where $\underline{\xi}^+$ refers to the upper boundary displacement and $\underline{\xi}^-$ is the lower boundary displacement. Referring to the local frame $\left(\underline{n}, \underline{t}, \underline{t}'\right)$, $\underline{\underline{k}}$ commonly takes the form:

$$\underline{\underline{k}} = k_n \underline{n} \otimes \underline{n} + k_t \left(\underline{t} \otimes \underline{t} + \underline{t}' \otimes \underline{t}' \right) \tag{2}$$

where k_n and k_t are respectively the normal and tangential stiffness components. These components are classically evaluated from laboratory test performed on material specimen with a single fracture. It should be observed that the particular case of discontinuities without stress transfer (here denominated by cracks) can be straightforwardly included in the above formulation by considering null that parameters. On the other hand, the solid matrix behavior is formulated by the relation between strains $\underline{\underline{\varepsilon}}$ and stresses $\underline{\underline{\sigma}}$ by the fourth-order stiffness tensor $\mathbb{C}^s$:

$$\underline{\underline{\sigma}} = \mathbb{C}^s : \underline{\underline{\varepsilon}} \tag{3}$$

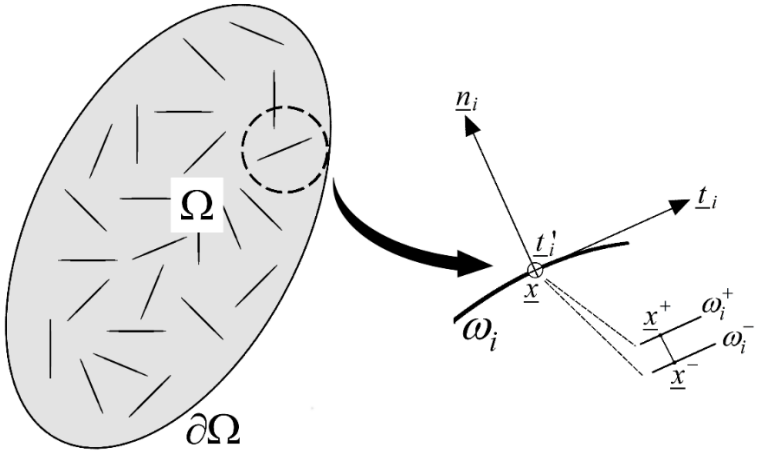

Figure 1: Fracture representation.

Micromechanical arguments evidence the macroscopic behavior is given by:

$$\underline{\underline{\Sigma}} = \mathbb{C}^{\text{hom}} : \underline{\underline{\text{E}}} \tag{4}$$

where $\underline{\underline{\Sigma}}$ and $\underline{\underline{\text{E}}}$ stand respectively for the macroscopic stresses and strains. $\mathbb{C}^{\text{hom}}$ is the equivalent stiffness tensor to the homogenized material.

Simplifying the fracture shape to an oblate spheroid (see Figure 2) with aspect ratio $\text{X} = c/a$ tending to zero (where $2c$ is the fracture aperture and a is the fracture radius), makes possible apply the Mori-Tanaka scheme in order to determine the homogenized stiffness $\mathbb{C}^{\text{hom}}$. Referring only to isotropic solid matrix behavior (where the solid matrix stiffness $\mathbb{C}^s = 3k^s \mathbb{J} + 2\mu^s \mathbb{K}$ is fully represented by its bulk k^s and shear μ^s moduli) and supposing isotropic fracture orientation, the

elastic stiffness tensor reads (Maghous et al. [4]):

$$\mathbb{C}^{\hom} = 3k^{\hom}\mathbb{J} + 2\mu^{\hom}\mathbb{K} \tag{5}$$

where $\mathbb{J} = 1/3\ \underline{\underline{1}} \otimes \underline{\underline{1}}$ and $\mathbb{K} = \mathbb{I} - \mathbb{J}$ are respectively the spherical and deviatoric projector tensors, $\underline{\underline{1}}$ is the second-order unity tensor, $\mathbb{I}$ is the fourth-order unity tensor and $\otimes$ refers to the tensorial product. The homogenized bulk $k^{\hom}$ and shear $\mu^{\hom}$ moduli read:

$$k^{\hom} = \frac{k^s}{1+\varepsilon\mathcal{M}_k} \quad \text{and} \quad \mu^{\hom} = \frac{\mu^s}{1+\varepsilon\mathcal{M}_\mu} \tag{6}$$

$\varepsilon = \mathcal{N}\,a^3$ is the fracture density parameter defined by Budiansky and O'Connel [5] connected to the fracture volumetric fraction $f = 4\pi\varepsilon \mathrm{X}/3$. $\mathcal{N}$ is the number of fractures per unit volume. The dimensionless parameters $\mathcal{M}_k(k^s, \mu^s, ak_n, ak_t)$ and $\mathcal{M}_\mu = (k^s, \mu^s, ak_n, ak_t)$ are:

$$\mathcal{M}_k = \frac{\frac{4}{3}\pi k^s/\mu^s}{\pi\kappa_1 + ak_n/\mu^s} \quad \text{and} \quad \mathcal{M}_\mu = \frac{16\pi\,\kappa_4}{15}\,\frac{6\kappa_2 + 4\kappa_3 + 9\pi\kappa_4\left(3\kappa_1+\kappa_4\right)}{\left(3\pi\kappa_1\kappa_4+\kappa_2\right)\left(4\kappa_3+9\pi\kappa_4(\kappa_1+\kappa_4)\right)} \tag{7}$$

where

$$\kappa_1 = \frac{3k^s+\mu^s}{3k^s+4\mu^s} \;;\; \kappa_2 = \frac{3k_n\,a}{3k^s+4\mu^s} \;;\; \kappa_3 = \frac{3k_t\,a}{3k^s+4\mu^s} \;;\; \kappa_4 = \frac{\mu^s}{3k^s+4\mu^s} \tag{8}$$

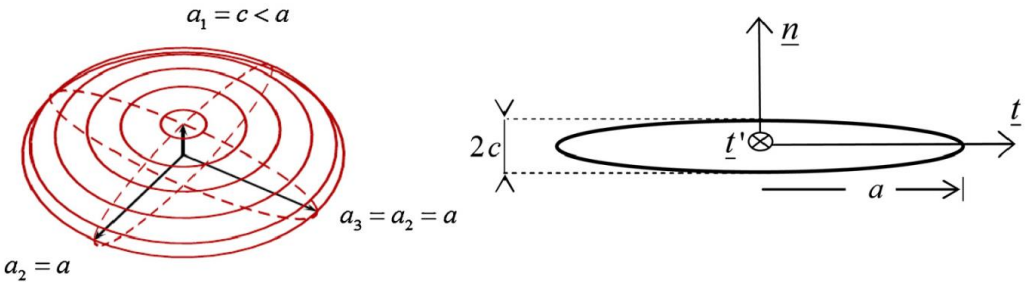

Figure 2: Ellipsoidal fracture representation

In order to obtain the propagation criterion dependent on viscous components, the homogenized elastic behavior have to be extended to the viscoelastic one. In this reasoning, the solid matrix and fracture behaviors read:

$$\underline{\underline{\sigma}} = \mathbb{R}^s \circ \underline{\underline{\varepsilon}} \quad \text{and} \quad \underline{T} = \underline{\underline{k}}^R \circ \left[\underline{\xi}\right] \tag{9}$$

The symbol $\mathbb{R}^s$ stands for the matrix's relaxation tensor and $\underline{\underline{k}}^R$ is the viscoelastic counterpart of the fracture stiffness $\underline{\underline{k}}$. The operator "$\circ$" stands for the hereditary convolution integral, which reads:

$$U(t,\tau)\circ V(t) = U(t,t)\bullet V(t) - \int_0^t \frac{\partial U(\mathrm{t},\tau)}{\partial\tau}\bullet V(\tau)\,\mathrm{d}\,\tau \tag{10}$$

where $\bullet$ define the order-compatible tensorial contraction such that the resulting operation maintains the tensorial order of the variable V. By means of the micromechanical theory, the viscoelastic mechanical relationship between macroscopic strains $\underline{\underline{\mathrm{E}}}$ and macroscopic stresses $\underline{\underline{\Sigma}}$ is given at the macroscopic scale by:

$$\underline{\underline{\Sigma}} = \mathbb{R}^{\hom} \circ \underline{\underline{\mathrm{E}}} \tag{11}$$

$\mathbb{R}^{\hom}$ corresponds to the effective relaxation tensor to the homogenized material. Making use of the correspondence principle, Aguiar and Maghous [1] have demonstrated that the homogenized relaxation tensor $\mathbb{R}^{\hom^*}(p)$ can be represented in the Laplace-Carson space as:

$$\mathbb{R}^{\hom^*} = 3k^{\hom^*}\mathbb{J} + 2\mu^{\hom^*}\mathbb{K} \quad \text{with} \quad k^{\hom^*} = \frac{k^{s^*}}{1+\varepsilon\mathcal{M}_k^*} \quad \text{and} \quad \mu^{\hom^*} = \frac{\mu^{s^*}}{1+\varepsilon\mathcal{M}_\mu^*} \tag{12}$$

where

$$\mathcal{M}_k^* = \frac{\frac{4}{3}\pi k^{s^*}/\mu^{s^*}}{\pi\kappa_1^* + a k_n^*/\mu^{s^*}} \quad \text{and} \quad \mathcal{M}_\mu^* = \frac{16\pi\,\kappa_4^*}{15}\frac{6\kappa_2^* + 4\kappa_3^* + 9\pi\kappa_4^*\left(3\kappa_1^* + \kappa_4^*\right)}{\left(3\pi\kappa_1^*\kappa_4^* + \kappa_2^*\right)\left(4\kappa_3^* + 9\pi\kappa_4^*(\kappa_1^* + \kappa_4^*)\right)} \tag{13}$$

and

$$\kappa_1^* = \frac{3k^{s^*} + \mu^{s^*}}{3k^{s^*} + 4\mu^{s^*}} \;\; ; \;\; \kappa_2^* = \frac{3k_n^* a}{3k^{s^*} + 4\mu^{s^*}} \;\; ; \;\; \kappa_3^* = \frac{3k_t^* a}{3k^{s^*} + 4\mu^{s^*}} \;\; ; \;\; \kappa_4^* = \frac{\mu^{s^*}}{3k^{s^*} + 4\mu^{s^*}} \tag{14}$$

The super index * indicates the functions are written at the Laplace-Carson domain in the p-time variable. Known the constituent (solid matrix and fractures) rheological behavior, the moduli k^{s^*}, μ^{s^*}, k_n^* and k_t^* can be straightly replaced by the corresponds functions written on Laplace-Carson domain. Supposing, for example, the solid matrix behaves as the Burger models and the fractures behaves as the Maxwell model (see figure 3):

$$k^{s^*}(p) = \left(\frac{1}{k_{e,M}^s} + \frac{1}{p\,k_{v,M}^s} + \frac{1}{k_{e,K}^s + p\,k_{v,K}^s}\right)^{-1} \text{ and } \mu^{s^*}(p) = \left(\frac{1}{\mu_{e,M}^s} + \frac{1}{p\,\mu_{v,M}^s} + \frac{1}{\mu_{e,K}^s + p\,\mu_{v,K}^s}\right)^{-1} \tag{15}$$

and

$$k_n^*(p) = \left(\frac{1}{k_{n,M}^e} + \frac{1}{p\,k_{n,M}^v}\right)^{-1} \text{ and } k_t^*(p) = \left(\frac{1}{k_{t,M}^e} + \frac{1}{p\,k_{t,M}^v}\right)^{-1} \tag{16}$$

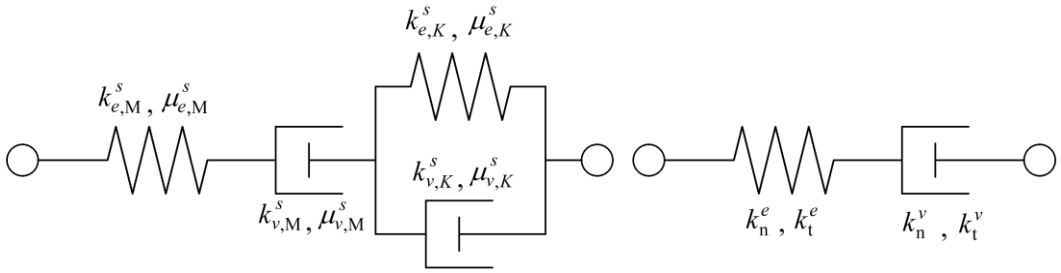

Figure 3: Burger matrix and Maxwell fracture representation

Making use of a specific procedure, Aguiar and Maghous [1] have demonstrated the homogenized relaxation moduli can be written through a particular generalized Maxwell model. This procedure requires the moduli $k^{\hom^*}$ and $\mu^{\hom^*}$, in the Laplace-Carson domain, be written as a quotient between polynomials:

$$k^{\hom^*}(p)=\frac{A^k(p)}{B^k(p)}=\frac{\sum_{n=0}^{g^k}a_n^k p^n}{\sum_{n=0}^{g^k}b_n^k p^n}=\frac{\sum_{n=0}^{g^k}a_n^k p^n}{\prod_{n=1}^{z^\mu}\left(p-r_n^k\right)^{g_n^k}} \tag{17}$$

and

$$\mu^{\hom^*}(p)=\frac{A^\mu(p)}{B^\mu(p)}=\frac{\sum_{n=0}^{g^\mu}a_n^\mu p^n}{\sum_{n=0}^{g^\mu}b_n^\mu p^n}=\frac{\sum_{n=0}^{g^\mu}a_n^\mu p^n}{\prod_{n=1}^{z^\mu}\left(p-r_n^\mu\right)^{g_n^\mu}} \tag{18}$$

Given $\alpha=k$ or μ, parameters a_n^α and b_n^α are the polynomials coefficients, g^α is the polynomial degree, r_n^α is the n-th B^α polynomial root, z^α is the number of main poles, g_n^α is the degree of n-indicated pole and p is the polynomial variable. Expressions (17) and (18) lead to the following expressions in the time domain [1]:

$$k^{\hom}(t)=\frac{a_0^k}{b_0^k}H(t)+\sum_{n=1}^{g^k}\frac{A^k(r_n^k)}{r_n^k\left.\frac{\partial B^k(p)}{\partial p}\right|_{p=r_n^k}}e^{r_n^k t}H(t) \tag{19}$$

and

$$\mu^{\hom}(t)=\frac{a_0^\mu}{b_0^\mu}H(t)+\sum_{n=1}^{g^\mu}\frac{A^\mu(r_n^\mu)}{r_n^\mu\left.\frac{\partial B^\mu(p)}{\partial p}\right|_{p=r_n^\mu}}e^{r_n^\mu t}H(t) \tag{20}$$

where $H(t)$ is the Heaviside function.

3 Fracture propagation criterion in viscoelasticity

Classically, the propagation criterion is developed based on thermodynamic concepts. Griffith [6] have firstly applied that concepts in order to formulate a propagation criterion to glassy materials. Ever since, many authors have extended that analysis in order to include other material kinds. Criterions formulated to time-dependent materials was extensively developed in the single-cracks context [7-14]. Recent approaches [15-16], however, used the micromechanical theory to address the micro-cracked issue. The following reasoning extends the propagation criterion by using the micro-fractured formulation developed previously.

3.1 Elastic Framework

Based on first and second thermodynamic laws, the classical linear elastic fracture mechanics suggests the energy dissipated ϕ^f on propagation mechanisms reads:

$$\phi^f=-\frac{\partial\psi}{\partial\ell}\dot{\ell} \tag{21}$$

where ψ stands for the elastic energy and ℓ is the crack length. Griffith [6] suggest that, during the crack propagation ($\dot{\ell}>0$), the energy dissipation reaches a limit value:

$$\phi^f\left(\dot{\ell}>0\right)=\mathcal{F}_c\dot{\ell}>0 \tag{22}$$

$\mathcal{F}_c$ corresponds to the material critical energy, being nowadays evaluated in laboratory tests. By expressions (21) and (22) becomes clear that $\partial\psi/\partial\ell$, commonly referred as energy release rate $\mathcal{F}$, assumes the role of thermodynamic force responsible for the propagation. The propagation criterion emerge from this insight, comparing the energy release rate with the critical energy in order to verify the crack propagation:

$$\mathcal{F}<\mathcal{F}_c\Rightarrow\dot{\ell}=0 \qquad \text{and} \qquad \mathcal{F}=\mathcal{F}_c\Rightarrow\dot{\ell}\geq 0 \tag{23}$$

This formulation accounts $\mathcal{F}$ as the only variable responsible for the crack propagation. In the elastic single-fracture context, the energy release rate reads:

$$\mathcal{F}=-\frac{1}{2}\underline{\underline{\varepsilon}}:\frac{\partial\mathbb{C}}{\partial\ell}:\underline{\underline{\varepsilon}}=\frac{1}{2}\underline{\underline{\sigma}}:\frac{\partial\mathbb{C}^{-1}}{\partial\ell}:\underline{\underline{\sigma}} \tag{24}$$

3.2 Viscoelastic propagation criterion to micro-fractures

Extending the thermodynamic-based analysis to viscoelastic micro-fractured materials, the energy dissipation ϕ can be expressed as:

$$\phi=-\frac{\partial\psi}{\partial\left\{\underline{\underline{\varepsilon}}^v\right\}}:\left\{\dot{\underline{\underline{\varepsilon}}}^v\right\}-\frac{\partial\psi}{\partial\varepsilon}\dot{\varepsilon} \tag{25}$$

where $\left\{\dot{\underline{\underline{\varepsilon}}}^v\right\}$ stands for the viscoelastic strain fields acting in the medium. Since the first right-hand-side term is related to viscous dissipation, it becomes possible write:

$$\phi_f=\phi-\phi^v=-\frac{\partial\psi}{\partial\varepsilon}\dot{\varepsilon} \quad \text{where} \quad \phi^v=-\frac{\partial\psi}{\partial\left\{\underline{\underline{\varepsilon}}^v\right\}}:\left\{\dot{\underline{\underline{\varepsilon}}}^v\right\} \tag{26}$$

However, in a macroscopic analysis, the single-point verification isn't sufficiently to evaluate the damage propagation, becoming necessary analyze all the VER by evaluating the effective energy dissipation to fracture propagation Φ_f.

$$\Phi_f=\left\langle\phi_f\right\rangle=-\left\langle\frac{\partial\psi}{\partial\varepsilon}\right\rangle\dot{\varepsilon} \tag{27}$$

The operator $\langle\bullet\rangle$ corresponds to the volumetric mean upon the REV. Assuming the VER volume Ω doesn't depending on ε:

$$\left\langle\frac{\partial\psi}{\partial\varepsilon}\right\rangle=\frac{\partial\left\langle\psi\right\rangle}{\partial\varepsilon}=\frac{\partial\Psi}{\partial\varepsilon} \tag{28}$$

where Ψ is the macroscopic elastic energy of the viscoelastic material. In a medium where the fracture is propagating $\left(\dot{\varepsilon}>0\right)$, the energy dissipation assumes a threshold value $\Phi_f=\mathcal{F}_v\dot{\varepsilon}>0$. It should be observed that differently from $\mathcal{F}_c$, which is a material property determined from laboratory test, $\mathcal{F}_v$ depending on the fracture density parameter. Dormieux et al. [17] have determined the following correspondence between $\mathcal{F}_c$ and $\mathcal{F}_v$:

$$\mathcal{F}_v=\frac{2\pi}{3}\left(\frac{\mathcal{N}}{\varepsilon}\right)^{1/3}\mathcal{F}_c \tag{29}$$

Once again, the effective energy release rate $\mathcal{F}$ assumes the role of the thermodynamic force responsible for the propagation:

$$\mathcal{F} = -\left.\frac{\partial \Psi}{\partial \varepsilon}\right|_{\underline{\underline{\mathrm{E}}},\left\{\underline{\underline{\varepsilon}}^{v}\right\}} \tag{30}$$

Combining the evidences which leads to the fracture propagation in a micro-fractured material, the criterion for propagation in viscoelasticity is written as:

$$\mathcal{F} < \mathcal{F}_v \Rightarrow \dot{\varepsilon} = 0 \qquad \text{and} \qquad \mathcal{F} = \mathcal{F}_v \Rightarrow \dot{\varepsilon} \geq 0 \tag{31}$$

Once again, the energy release rate $\mathcal{F}$ accounts as the only variable responsible for the fracture propagation. The main difference between expressions (23) and (31) corresponds to the elastic energy expression which writes the energy release rate.

3.3 Energy release rate

Starting from the rheological models describing the microscopic behaviors for the solid matrix and fractures, it becomes possible deduct the macroscopic elastic energy Ψ by the microscopic one. Assuming, by simplicity, both solid matrix and fractures may be represented by the Burger model, the microscopic expression to the elastic energy reads:

$$\psi = \frac{1}{2}\underline{\underline{\varepsilon}}_M^e : \mathbb{C}_M : \underline{\underline{\varepsilon}}_M^e + \frac{1}{2}\underline{\underline{\varepsilon}}_K^e : \mathbb{C}_K : \underline{\underline{\varepsilon}}_K^e \quad \text{with} \quad \mathbb{C}_\beta = \begin{cases} \mathbb{C}_\beta^s & \text{in} \quad \Omega \setminus \omega \\ \mathbb{C}_\beta^f & \text{in} \quad \omega \end{cases} \tag{32}$$

where β represents the Maxwell M or Kelvin K parts from the respective Burger models. $\mathbb{C}_\beta^s$ is the solid matrix stiffness tensor of beta's Burger part and $\mathbb{C}_\beta^f$ corresponds to the fourth-order fracture tensor of beta's Burger part related to the viscoelastic fracture stiffness $\underline{\underline{k}}^v$ [1]. $\underline{\underline{\varepsilon}}_\beta^e$ stands for the strain acting on the respective model spring.

Considering some basic Burger's relations ($\underline{\underline{\varepsilon}}_M^e = \underline{\underline{\varepsilon}}^e$, $\underline{\underline{\varepsilon}}_K^e = \underline{\underline{\varepsilon}}_K$ and $\mathbb{C}_M = \mathbb{R}_0$), it becomes possible write ψ as:

$$\psi = \frac{1}{2}\underline{\underline{\varepsilon}}^e : \mathbb{R}_0 : \underline{\underline{\varepsilon}}^e + \frac{1}{2}\underline{\underline{\varepsilon}}_K : \mathbb{C}_K : \underline{\underline{\varepsilon}}_K \quad \text{with} \quad \mathbb{R}_0 = \begin{cases} \mathbb{R}_0^s & \text{in} \quad \Omega \setminus \omega \\ \mathbb{R}_0^f & \text{in} \quad \omega \end{cases} \tag{33}$$

By definition, on micromechanical arguments, the macroscopic elastic energy is the volumetric integral over the local free energy, being written as:

$$\Psi = \langle \psi \rangle = \frac{1}{2}\left\langle \underline{\underline{\varepsilon}}^e : \mathbb{R}_0 : \underline{\underline{\varepsilon}}^e \right\rangle + \frac{1}{2}\left\langle \underline{\underline{\varepsilon}}_K : \mathbb{C}_K : \underline{\underline{\varepsilon}}_K \right\rangle \tag{34}$$

Based on micromechanical reasoning, it is possible demonstrate that:

$$\Psi = \Psi_I + \Psi_R + \Psi_K \tag{35}$$

where the instantaneous energy Ψ_I, the residual energy Ψ_R and the Deferred (or Kelvin's) part energy Ψ_D can be represented by

$$\Psi_I = \frac{1}{2}\left(\underline{\underline{\mathrm{E}}} - \underline{\underline{\mathrm{E}}}^v\right) : \mathbb{R}_0^{\hom} : \left(\underline{\underline{\mathrm{E}}} - \underline{\underline{\mathrm{E}}}^v\right) \tag{36}$$

$$\Psi_R = \frac{1}{2}\left\langle \left(\underline{\underline{\varepsilon}}^R - \underline{\underline{\varepsilon}}^v\right) : \mathbb{R}_0 : \left(\underline{\underline{\varepsilon}}^R - \underline{\underline{\varepsilon}}^v\right) \right\rangle \tag{37}$$

$$\Psi_D = \frac{1}{2}\left\langle \underline{\underline{\varepsilon}}_K : \mathbb{C}_K : \underline{\underline{\varepsilon}}_K \right\rangle \tag{38}$$

$\underline{\underline{\varepsilon}}^R$ is the residual strain field which remains in the material at the end of an instantaneous discharge

$\underline{\underline{\Sigma}} = 0$ and the microscopic $\underline{\underline{\varepsilon}}^v$ and macroscopic $\underline{\underline{E}}^v$ viscous strains are defined by:

$$\underline{\underline{\varepsilon}}^v = \mathbb{R}_0^{-1} : \int_0^t \frac{\partial \mathbb{R}(t,\tau)}{\partial \tau} : \underline{\underline{E}}(\tau)\, d\tau \quad \text{and} \quad \underline{\underline{E}}^v = \mathbb{R}_0^{\text{hom}^{-1}} : \int_0^t \frac{\partial \mathbb{R}^{\text{hom}}(t,\tau)}{\partial \tau} : \underline{\underline{E}}(\tau)\, d\tau \tag{39}$$

Since the analysis focus demands on $\partial\Psi/\partial\varepsilon$, and not directly on Ψ , it is possible demonstrate that:

$$\left.\frac{\partial \left\langle \underline{\underline{\varepsilon}}_K : \mathbb{C}_K : \underline{\underline{\varepsilon}}_K \right\rangle}{\partial \varepsilon}\right|_{\left\{\underline{\underline{\varepsilon}}^v\right\}} = 0 \tag{40}$$

Besides that, with the aid of micromechanics tools, the residual energy can be reformulated as:

$$\Psi^R = \frac{1}{2}\underline{\underline{\Sigma}} : \underline{\underline{E}}^v - \frac{1}{2}\left\langle \underline{\underline{\sigma}} : \underline{\underline{\varepsilon}}^v \right\rangle_\Omega \tag{41}$$

In particular cases where $\underline{\underline{\varepsilon}}^v$ is geometrically compatible, it is possible demonstrate that $\Psi^R = 0.$ Neglecting $\partial \underline{\underline{E}}^v / \partial\varepsilon$ [18] and supposing $\underline{\underline{\varepsilon}}^v$ geometrically compatible, the energy release rate reads:

$$\mathcal{F} = -\frac{\partial \Psi}{\partial \varepsilon} = -\frac{1}{2}\left(\underline{\underline{E}} - \underline{\underline{E}}^v\right) : \frac{\partial \mathbb{R}_0^{\text{hom}}}{\partial \varepsilon} : \left(\underline{\underline{E}} - \underline{\underline{E}}^v\right) = \frac{1}{2}\underline{\underline{\Sigma}} : \frac{\partial \mathbb{R}_0^{\text{hom}^{-1}}}{\partial \varepsilon} : \underline{\underline{\Sigma}} \tag{42}$$

Since the homogenized relaxation tensor is macroscopically isotropic, the energy release rate expression can be rewritten in the indicial notation as:

$$\begin{aligned} \mathcal{F} = &-\frac{1}{2}\left(\frac{k_0^{\text{hom}^{-2}}}{9}\frac{\partial k_0^{\text{hom}}}{\partial \varepsilon} + \frac{\mu_0^{\text{hom}^{-2}}}{3}\frac{\partial \mu_0^{\text{hom}}}{\partial \varepsilon} \right)\left(\Sigma_{11} + \Sigma_{22} + \Sigma_{33}\right)^2 + \\ &-\frac{\mu_0^{\text{hom}^{-2}}}{4}\frac{\partial \mu_0^{\text{hom}}}{\partial \varepsilon}\left(\Sigma_{12}^2 + \Sigma_{13}^2 + \Sigma_{23}^2 - 2\Sigma_{11}\Sigma_{22} - 2\Sigma_{11}\Sigma_{33} - 2\Sigma_{22}\Sigma_{33}\right) \end{aligned} \tag{43}$$

or, calling $\underline{\underline{E}}^e = \underline{\underline{E}} - \underline{\underline{E}}^v$:

$$\begin{aligned} \mathcal{F} = &-\frac{1}{2}\left(\frac{\partial k_0^{\text{hom}}}{\partial \varepsilon} + \frac{4}{3}\frac{\partial \mu_0^{\text{hom}}}{\partial \varepsilon} \right)\left(\mathrm{E}_{11}^e + \mathrm{E}_{22}^e + \mathrm{E}_{33}^e\right)^2 + \\ &-\frac{\mu_0^{\text{hom}^{-2}}}{4}\frac{\partial \mu_0^{\text{hom}}}{\partial \varepsilon}\left(\mathrm{E}_{12}^{e\,2} + \mathrm{E}_{13}^{e\,2} + \mathrm{E}_{23}^{e\,2} - 2\mathrm{E}_{11}^e\mathrm{E}_{22}^e - 2\mathrm{E}_{11}^e\mathrm{E}_{33}^e - 2\mathrm{E}_{22}^e\mathrm{E}_{33}^e\right) \end{aligned} \tag{44}$$

Given the relationship between $\underline{\underline{\Sigma}}$ and $\underline{\underline{E}}$, both expressions (43) and (44) may be used, independently from the kind of applied load ($\underline{\underline{E}}$ or $\underline{\underline{\Sigma}}$).

4 Numerical Applications

Known the propagation criterion (31) as well as the energy release rate expression (43) or (44), it becomes helpful shows some numerical results obtained from this reasoning. The mechanical behavior attached to constituents (matrix and fractures) follows that one described in Figure 3. The parameter's value adopted to Burger matrix (in $\{GPa\}$ and $\{GPa\}\bullet\{ano\}$) and to Maxwell fractures (in $\{GPa\}/\{m\}$ and $\{GPa\}\bullet\{ano\}/\{m\}$) are:

$$\begin{aligned} k^s_{\mathrm{e},M} &= 24.4 \;\; ; \;\; k^s_{\mathrm{v},M} = 23.2 \;\; ; \;\; k^s_{\mathrm{e},K} = 39.3 \;\; ; \;\; k^s_{v,K} = 1.6 \\ \mu^s_{\mathrm{e},M} &= 13.3 \;\; ; \;\; \mu^s_{\mathrm{v},M} = 12.3 \;\; ; \;\; \mu^s_{\mathrm{e},K} = 14.1 \;\; ; \;\; \mu^s_{v,K} = 0.4 \\ k^e_{\mathrm{n}} &= 42.2 \;\; ; \;\; k^v_{\mathrm{n}} = 22.2 \;\; ; \;\; k^e_t = 16.9 \;\; ; \;\; k^v_t = 8.9 \end{aligned} \tag{45}$$

Defining the applied load by isotropic macroscopic strains $\underline{\underline{\mathrm{E}}} = \mathrm{E}(t)\,\underline{\underline{1}}$ and given the expression (11), the resultant macroscopic stresses are given by $\underline{\underline{\Sigma}} = \Sigma(t)\,\underline{\underline{1}}$, with $\Sigma(t) = 3k^{\mathrm{hom}} \circ \mathrm{E}$. This loading case leads to following energy release rate expression:

$$\mathcal{F} \;=\; -\frac{1}{2}\mathrm{E}^{e^2}\frac{\partial k_0^{\mathrm{hom}}}{\partial \varepsilon} \;=\; -\frac{1}{2}\frac{\Sigma^2}{k_0^{\mathrm{hom}^2}}\frac{\partial k_0^{\mathrm{hom}}}{\partial \varepsilon} \tag{46}$$

Applying constant strain loads $E(t) = \mathrm{E}_0\, H(t)$ under expression (46), the evolution of energy release rate is given by:

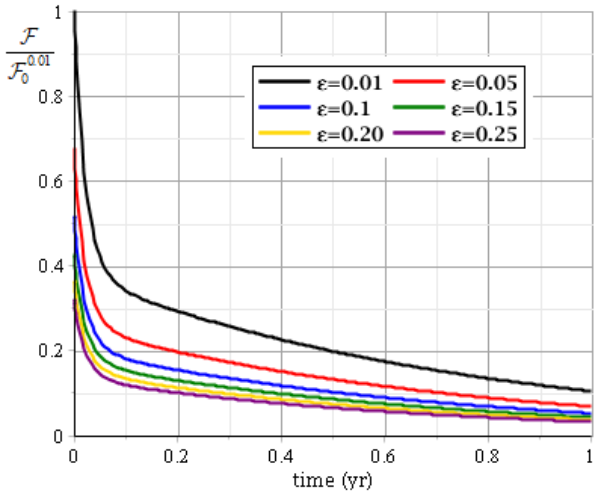

Figure 4: Energy release rate to constant strain loads

$$\mathcal{N} = 1;\; E_0 = 10^{-3};\; \mathcal{F}_0^{0.01} = \mathcal{F}\left(t = 0, \varepsilon = 0.01\right)$$

Regarding the constant strains, it is observed that the highest values for energy release rate occur at the initial instants, evidencing that elastic phenomena components control the fracture propagation. Even so, high value of damage parameter leads to lower energy release rates, leading to greater difficulty in the fracture propagation. This behavior is explained, for strain loads, due to the higher deformability introduced by the fractures to the homogenized medium.

On the other hand, applying constant strain rate in the form $E(t) = \dot{\mathrm{E}}_0\, t\, H(t)$ leads to the following energy release rate evolution:

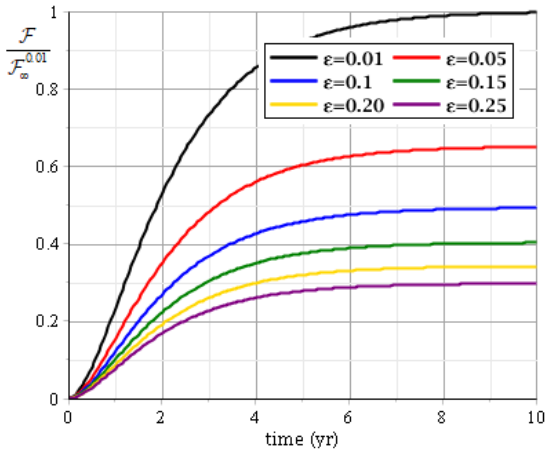

Figure 5: Energy release rate to constant strain loads

$$\mathcal{N}=1;\ \dot{\mathrm{E}}_0=10^{-3}\,yr^{-1};\mathcal{F}_\infty^{0.01}=\mathcal{F}\left(t=\infty,\varepsilon=0.01\right)$$

Differently from the elastic reasoning, which leads to a parabolic increasing-in-time function, the viscoelastic reasoning drive the energy release rate to a maximum-asymptotic increasing function. The asymptotic value is referred as $\mathcal{F}_\infty$ and can be used in an alternative propagation criterion. Comparing $\mathcal{F}_\infty$ with $\mathcal{F}_v$ leads to a time-independent criterion to evaluate the fracture propagation:

$$\begin{aligned}&\mathcal{F}_\infty\le\mathcal{F}_v\ \rightarrow \text{there isn't fracture propagation}\\&\mathcal{F}_\infty>\mathcal{F}_v\ \rightarrow \text{there is fracture propagation}\end{aligned}\tag{47}$$

Since $\mathcal{F}_\infty$ is evaluated from the initial damage parameter, depending on starter conditions the damage never will propagate. However, in the cases where the propagation will occurs, the instant of propagation start t_p can be evaluated from $\mathcal{F}(t_p)=\mathcal{F}_v$. The expression of asymptotic energy release rate can be evaluated by taking the limit of expression (46) when $t\rightarrow\infty$:

$$\mathcal{F}_\infty\ =\ -\frac{1}{2}\mathrm{E}_\infty^{e^2}\frac{\partial k_0^{\mathrm{hom}}}{\partial\varepsilon}\ =\ -\frac{1}{2}\frac{\Sigma_\infty^2}{k_0^{\mathrm{hom}^2}}\frac{\partial k_0^{\mathrm{hom}}}{\partial\varepsilon}\tag{48}$$

Given the constant strain rate and the relationship between macroscopic strains and stresses, expression (48) can be reformulated as:

$$\mathcal{F}_\infty\ =\ \frac{9}{2}\dot{\mathrm{E}}_0^2\frac{{k_{s,M}^v}^2}{k_{s,M}^{e^2}}\frac{{\mathcal{M}_k^0}^2}{\left(1+\varepsilon\mathcal{M}_k^\infty\right)^2}\left(\frac{k_{s,M}^e}{\mathcal{M}_k^0}-\frac{a\,k_{n,M}^e}{4\pi}\right)=\frac{1}{2}\Sigma_\infty^2\frac{{\mathcal{M}_k^0}^2}{k_{s,M}^e}\left(\frac{k_{s,M}^e}{\mathcal{M}_k^0}-\frac{a\,k_{n,M}^e}{4\pi}\right)\tag{49}$$

where

$$\mathcal{M}_k^0=\frac{\frac{4}{3}\pi\frac{k_{s,M}^e}{\mu_{s,M}^e}}{\pi\kappa_1^e+a\frac{k_{\mathrm{n},M}^e}{\mu_{s,M}^e}}\ ;\ \kappa_1^e=\frac{3k_{\mathrm{s},M}^e+\mu_{\mathrm{s},M}^e}{3k_{\mathrm{s},M}^e+4\mu_{\mathrm{s},M}^e}\ ;\mathcal{M}_k^\infty=\frac{\frac{4}{3}\pi\frac{k_{s,M}^v}{\mu_{s,M}^v}}{\pi\kappa_1^\infty+a\frac{k_{\mathrm{n},M}^v}{\mu_{s,M}^v}}\ ;\ \kappa_1^\infty=\frac{3k_{s,M}^v+\mu_{s,M}^v}{3k_{s,M}^v+4\mu_{s,M}^v}\tag{50}$$

In order to better comprehend the condition (47), two graphics are plotted. The first one presenting both $\mathcal{F}_\infty$ and $\mathcal{F}_v$, and the second one presenting the relative difference between its values in function of the critical energy:

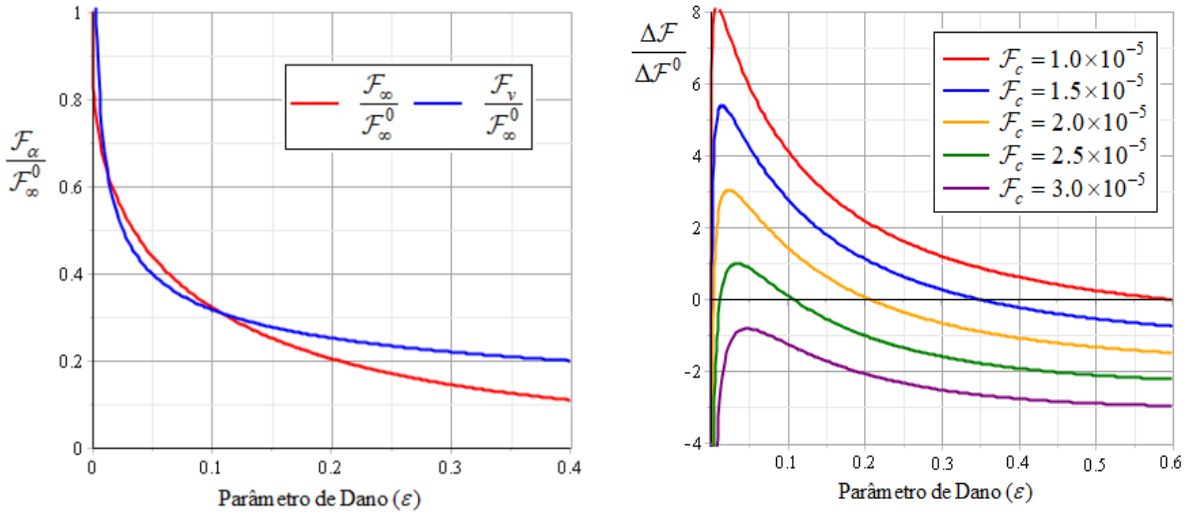

Figure 6: Comparison between asymptotic energy release rate and critical energy

$$\mathcal{N}=1;\ \dot{\mathrm{E}}_0 = 10^{-3}\,yr^{-1};\ \mathcal{F}_c = 2.0\times10^{-5};\ \mathcal{F}_\infty^0 = \mathcal{F}\left(t=\infty, \varepsilon = 10^{-5}\right);\ \Delta\mathcal{F} = \mathcal{F}_\infty - \mathcal{F}_v;$$

$$\Delta\mathcal{F}^0 = \Delta\mathcal{F}\left(\varepsilon = 10^{-5}, \mathcal{F}_c = 2.0\times10^{-5}\right)$$

That Figure suggest there is an interval of ε where the fracture is possible ($0.004 < \varepsilon < 0.207$ to the used dates). If the material is too intact or too damaged, the asymptotic energy release rate doesn't achieve the critical energy and the fracture won't propagate. If the value of the initial damage parameter is located within the given range, at some point $t < \infty$ the energy release rate will reach the value of the critical energy and, since $\mathcal{F} > \mathcal{F}_c$ is not physically possible, the fracture propagation will occur until equilibrium (or the total rupture) is reestablished.

The upper interval damage parameter is referred as $\varepsilon_\infty^{\min}$ and, supposing the damage evolution is sufficiently slow allowing a certain mechanical equilibrium at each stage during propagation, this value balance the asymptotic energy release rate and critical energy on the system, leading to the propagation end. That value is understand as the "minimum final damage parameter" since if the mechanical equilibrium during the damage evolution doesn't occurs the expected damage parameter is necessarily higher than $\varepsilon_\infty^{\min}$.

An alternative propagation condition also can be formulated in strains or stresses conditions. In a critical domain, expression (46) can be reformulated in order to express the critical strain or critical stress necessary to the fracture propagation:

$$\mathrm{E}_c^e = \frac{\Sigma_c}{k_0^{\hom}} = \sqrt{-2\mathcal{F}_v\left(\frac{\partial k_0^{\hom}}{\partial\varepsilon}\right)^{-1}} \tag{51}$$

Expression (51) can be used to time-dependent expression comparing $\mathrm{E}^e \le \mathrm{E}_c^e$ or $\Sigma \le \Sigma_c$. This expression analyze time-by-time if the propagation starts at the current moment. Resorting to constant strain rate loads, the critical strain rate $\dot{\mathrm{E}}_0^{CR}$ or critical asymptotic values of Σ_∞^{CR} can be used as propagation criterion. Comparing expression (48) to $\mathcal{F}_v$ in a critical domain ($\mathcal{F}_\infty = \mathcal{F}_v$)

$$\Sigma_\infty^{CR} = k_0^{\hom}\sqrt{-2\mathcal{F}_v\left(\frac{\partial k_0^{\hom}}{\partial\varepsilon}\right)^{-1}} = 3\dot{\mathrm{E}}_0^{CR}\frac{k_{s,M}^v}{1+\varepsilon\mathcal{M}_k^\infty} \tag{52}$$

while $\Sigma_\infty \le \Sigma_\infty^{CR}$ or $\dot{\mathrm{E}}_0 \le \dot{\mathrm{E}}_0^{CR}$ there aren't fracture propagation. Otherwise, if $\Sigma_\infty > \Sigma_\infty^{CR}$ or

$\dot{E}_0 > \dot{E}_0^{CR}$, the applied load leads to the fracture propagation starting in an undefined transient time. Figure 7 present the critical strain rate in function of the damage parameter and critical energy. Observes that, to $\dot{E}_0 = 10^{-3}\, yr^{-1}$ and $\mathcal{F}_c = 2\times10^{-5}$ the same damage parameter interval induce the fracture propagation.

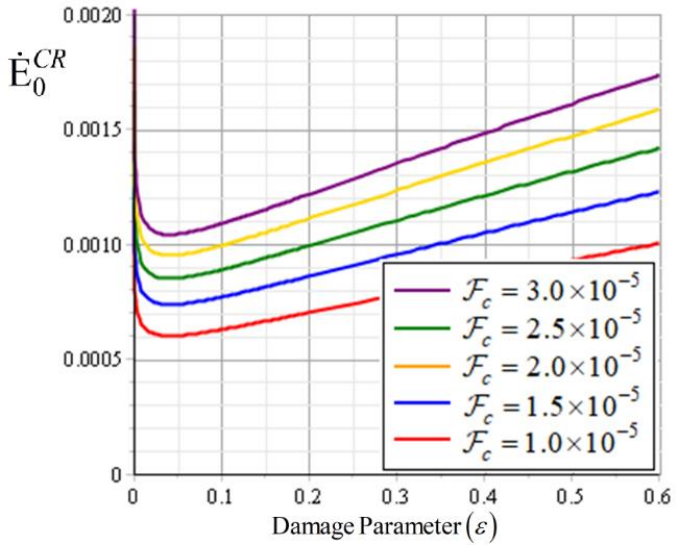

Figure 7: Critical strain rate in function of damage parameter and critical energy $\mathcal{N} = 1$;

Based on reasoning developed to energy release rate (Figure 5) and to the comparison between critical energy and asymptotic energy release rate (Figure 6), becomes possible extract the propagation initiation time as well as an estimative (the minimum value) of final damage parameter. Figure 8 in the sequence shows the evolution of energy release rate before the propagation start (blue line) and after the propagation end (red line). It is important observe that, the energy release rate between the propagation start and end depends on the propagation model adopted to the analysis. Propagation models aren't the scope of this work. The continuous line indicate the expected behavior of the material in each propagation step and the dash line indicate the fictitious behavior supposing there aren't fracture propagation.

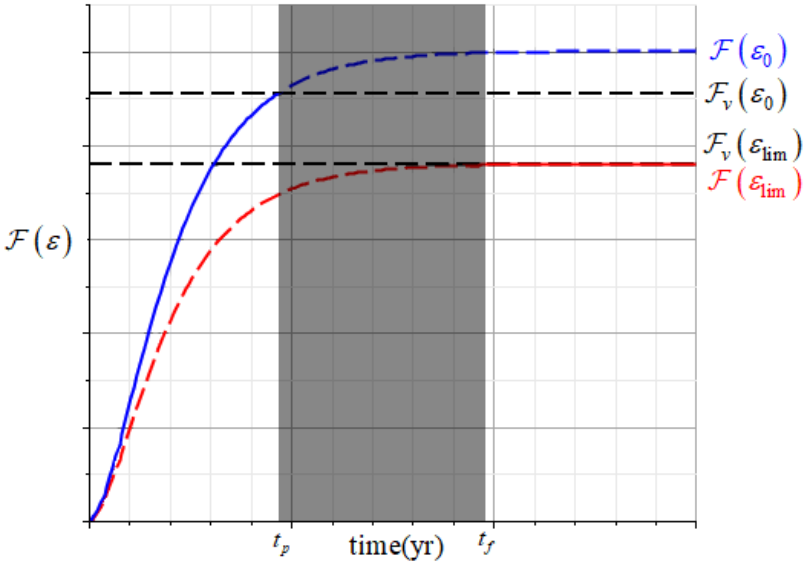

Figure 8: Energy release rate to constant strain loads

The Figure 8 distinguish 3 distinct intervals. In the first one interval $\left(0 \le t \le t_p\right)$ the critical energy is higher than the energy release rate and $\mathcal{F}\left(\varepsilon_0\right)$ increases from zero to $\mathcal{F}_v\left(\varepsilon_0\right)$, on that condition there isn't fracture propagation. On the limit time t_p the propagation criterion is achieved and consequently the propagation starts. The time t_p where the propagation criterion is achieved is called initiation time.

The second one interval $\left(t_p \le t \le t_f\right)$ is marked by the fracture propagation, where at first the damage parameter increases from ε_0 to $\varepsilon_\infty^{\min}$. In this interval, the fracturing process occur, opening space to the fracture models be included. Once ε reaches $\varepsilon_\infty^{\min}$, the asymptotic energy release rate $\mathcal{F}_\infty\left(\varepsilon_{\lim}\right)$ match with the critical energy $\mathcal{F}_v\left(\varepsilon_{\lim}\right)$ and, consequently the propagation criterion becomes inactive, stopping the fracture propagation. The exact localization of the time t_f where the propagation stop depend on the propagation model and speed.

In the last interval we have $\mathcal{F}\left(\varepsilon_{\lim}\right) = \mathcal{F}_v\left(\varepsilon_{\lim}\right)$ in a constant asymptotic baseline. That interval is marked by the one-way instability, where increases on strain rate lead to more fracture propagation and decreases on strain rate will keep the same damage level, lowering the energy release rate. In problems where the fracture propagation is catastrophic this interval doesn't occurs because the material brakes before that. It should be observed that, if the mechanical balance during the propagation isn't achieved, the load increases doesn't leads necessarily to more fracture propagation.

5 Conclusions

Simplifying the fracture interface model to oblate spheroids with aspect ratio tending to zero (slim shape) and keeping the fracture ability of transfer normal and tangential efforts (through the associated behavior which relates the stress vector to the displacement jump), it becomes possible uses the Mori-Tanaka schemes in order to formulate the homogenized elastic stiffness tensor. The elastic formulation associated to the correspondence principle allows us to obtain the viscoelastic homogenized relaxation tensor.

Extending the classical thermodynamic framework to the viscoelastic reasoning a propagation criterion was formulated. Similarly to Griffith's work, the criterion compares the energy release rate with a critical value to evaluate the propagation existence. The energy release rate is evaluated from the derivative of free energy with respect to the fracture density parameters, which represents macroscopically the fracture amount. In this way, the macroscopic free energy was determined starting from the microscopic one and them, applied to the energy release rate.

Numerical applications show that the energy release rate depending directly from the load. In the case where strain loads are instantly applied, the fracture propagation was controlled by elastic phenomena. Even so, high value of damage parameter leads to lower energy release rates, leading to greater difficulty in the fracture propagation. In the case where constant strain rates was applied, the energy release rate increases from zero to an asymptotic maximum value, making clear the viscoelastic behavior participation. Since it is possible stablishes the asymptotic energy release rate to the initial damage parameter, its value can be compared to the critical energy in order to formulate a time-independent propagation criterion. In addition to providing information about the propagation possibility, this relation allows to determine a ready-to-propagate interval where the propagation will occur and a minimum lower limit for the damage parameter at the end of propagation. Alternative propagation criterion formulated in terms of strains or stresses also was formulated. These relations lead to the same ready-to propagate interval by comparing the applied load to the respective critical value.

Some key issues still need to be foreseen in the future:

- First of all, should be kept in mind that validation of the theoretical modeling against experimental data either from laboratory or field measurements remains to be assessed. Due to the lack in available data regarding the specific time-dependent behavior of fractures, a suitable strategy would rely upon an inverse analysis to identify beforehand the viscoelastic properties of the constituents (matrix and fractures) from direct comparisons between experimental tests performed on the fractured material and the micromechanical predictions.

• The analysis has been restricted to micro-fractures, which by definition are fractures much smaller than the REV size. However, some materials such as rock masses can exhibit long scale discontinuities (long fractures), crosscutting the REV. Since this fractures can't be viewed from the micromechanical viewpoint, the long fracture propagation should be evaluated separately.

• The propagation speed can affect directly the propagation mechanisms. On the one hand, fast fracture propagation presents a behavior similar to glassy materials, propagating all damage instantly when the critical energy is reached. On the other hand, in slow fracture propagation the final configuration can take time to be reached, may not occurring if the material is unloaded. That model differences can lead to transient efforts, which change the limit damage parameter.

References

[1] C. B. Aguiar and S. Maghous. Micromechanical approach to effective viscoelastic properties of micro-fractured geomaterials. *International Journal for Numerical and Analytical Methods in Geomechanics*. vol. 47, n. 16, pp. 1-29, 2018

[2] R. E. Goodman. Methods of Geological Engineering in Discontinuous Rocks. *West Publishing*. 1st ed, 1976.

[3] S. C. Bandis, A. C. Lumsden and N. R. Barton. Fundamentals of Rock Joint Deformation. *International Journal of Rock Mechanics and Mining & Geomechanics Abstracts*. vol. 20, n. 6, pp. 249-268, 1983.

[4] S. Maghous, G. Lorenci and E. Bittencourt. Effective poroelastic behavior of a jointed rock. *Mechanics Research Communications*. vol. 509, pp. 54-69, 2014.

[5] B. Budiansky and R. J. O'Connel. Elastic moduli of a cracked solid. *International Jounal of Solids Structures*. vol. 12, pp. 91-97, 1976.

[6] A. A. Griffith. The phenomenon of rupture and flow in solids. *Philosophical Transactions of the Royal Society of London. A.* vol. 221, pp. 163-198, 1921.

[7] J. R. Willis. Crack Propagation in viscoelastic media. *Journal of the Mechanics and Physics of Solids*. vol. 15, pp. 229-240, 1967.

[8] W. G. Knauss and H. Dietmann. Crack propagation under variable load histories in linearly viscoelastic solids. *International Journal of Engineering Science*. vol. 8, n. 8, pp. 643-656, 1970.

[9] R. A. Schapery. A theory of crack initiation and growth in viscoelastic media: I. Theoretical development. *International Journal of Fracture*. vol. 11, n. 1, pp. 141-159, 1975.

[10] R. M. Christensen and E. M. Wu. A theory of crack growth in viscoelastic materials. *Engineering Fracture Mechanics*. vol. 14, pp. 2315-225, 1981.

[11] J. R. Masueiro and G. J. Creus. Finite elements analysis of viscoelastic fracture. *International Journal of Fracture*. vol. 60, n. 3, pp. 269-282, 1993.

[12] R. Y. Liang and J. Zhou. Energy based approach for crack initiation and propagation in viscoelastic solids. *Engineering Fracture Mechanics*. vol. 58, n. ½, pp. 71-85, 1997.

[13] F. Dubois, C. Chazal and C. Petit. Modelling of crack growth initiation in a linear viscoelastic material. *Journal of Theoretical and Applied Mechanics*. vol. 37, n. 2, pp. 207-222, 1999.

[14] B. N. J. Persson and E. A. Brener. Crack propagation in viscoelastic solids, *Physical Reviwer E*. vol. 71, n. 3, pp. 1-8, 2005.

[15] S. T. Nguyen, L. Jeannin, L. Dormieux and F. Renard. Fracturing of viscoelastic geomaterials and application to sedimentary layered rocks. *Mechanics Research Communications*. vol. 49, pp. 50-56, 2013.

[16] S. T. Nguyen and L. Dormieux. Propagation of micro-cracks in viscoelastic materials: Analytical and numerical methods. *International Journal of Damage Mechanics*. vol. 24, n. 4, pp. 562-581, 2014.

[17] l. Dormieux, D. Kondo and F.-J. Ulm. Microporomechanics. *JohnWiley & Sons*, 1st ed, 2006.

[18] S. T. Nguyen, L. Dormieux, Y. Le Pape and J. Sanhuja. Crack propagation in viscoelastic structures: Theoretical and numerical analyses. *Computational Materials Sciences*. vol. 50, pp. 83-91, 2010.